MINISTRY OF EDUCATION AND TRAINING
VIET NAM INSTITUTE OF INDUSTRIAL CHEMISTRY
****

NGUYEN THI PHUONG HOA

STUDY ON PREPARATION, MODIFY AND CHARACTERIRATION OF Pt/GRAPHENE APPLICATION IN DMFC

Specialization: Theoretical Chemistry and Physical Chemistry
Code: 62.44.01.19

SUMMARY OF CHEMICAL PhD.THESIS

Hanoi, 2015

The thesis completed at:

Vietnam Institue of Industrial Chemistry

Scientific Advisors: 1. Assoc. Prof. Dr. Vu Thi Thu Ha

2. Assoc. Prof. Dr. Nguyen Dinh Lam

Reviewer 1: ………………………………………………………

Reviewer 2: ………………………………………………………

Reviewer 3: ………………………………………………………

The thesis will be defended at Institue level Council of thesis assesment at Vietnam Institue of Industrial Chemistry

Time: ……. date …….. month……. year

The thesis could be found at:

Vietnam National Library

A – INTRODUCTION

1. Reasons to choose the subject

Graphene, a single layer of carbon atoms, the material crystallized two-dimensional (2D) hexagonal structure complete week thin layer with a thickness of one atom of carbon, about 1 to 1.6 nm, which is the material considered as the thinnest of all types of materials. This is an ultra-thin material, super flat, good thermal conductivity and electrical conductivity and high stability.

With its unusual properties, graphene is potentially broad applications in many different fields: energy storage, energy production, biotechnology, biomedical, materials, ... particularly in the field of catalyst, graphene is a promising attractive material, especially in the oxidation and electrochemical.

In the context of fossil energy resources are dwindling, the world will face an energy crisis is occurring at a global scale. Currently, developed countries such as Canada, France, America, ... has made the different fuel cell types to ensure energy service sectors such as information technology, transportation, science school universe ... But in our country, fuel cell still is a quite new type of energy. Therefore, the research direct to develop a new catalytic system to transform chemical energy into electrical energy for fuel cell applications is a right direction in the development strategy of Vietnam's energy sector.

According to the study results were announced, the precious metal catalysts, including Pt, carry on graphene support (Pt/G) expressed suporiority role than Pt traditional block catalysts or Pt catalysts carried on supports such as carbon black, carbon nano tubes. On this basis, the concerned research directions are to find new methods of graphene synthesis, functionalized graphene and dispersed Pt on the nanoscale up to graphene, modified catalytic Pt/G to improve properties and durability of the catalytic activity of electrochemical catalysts applied in fuel cells used direct methanol (DMFC).

2. Objects and contents

Successfully study on the process for preparing precious metal catalysts carried on graphene (new material ultra-thin, ultra-flat, good thermal conductivity and electrical conductivity and high stability), applied in fuel cells used direct methanol (DMFC).

To achieve this goal the main research contents of the thesis include:

- Study on synthesis graphene and catalyst based on Pt/rGO by various methods;
- Study on modyfication of catalysts based on Pt/rGO by different denaturant thereby select suitable catalysts and study on coating catalytic material on the surface of the electrode;
- Surveying the effect of work environment to work efficiently and durability of catalytic coated electrode;
- Experiment DMFC models.

3. The scientific and practice meanings of the thesis

The thesis synthesized catalyst Pt- 7% ASG (catalyst base on Pt carried on graphene which modified by oxide complex AlOOH and SiO_2) has high activity and especially durable activity in the electrochemical oxidation of methanol reaction, suitable as a catalyst in fuel cells DMFC made significantly reduce amount of precious metals used in catalysts, resulting in lower cost of DMFCs.

4. The new contributions of the thesis

- Systematic survey of different surfactants to synthesize few layer graphene (FLG) by mechanical delamination. These results show that CTAB and SDBS surfactants are two highly effective surfactants in the synthesis and dispersion FLG, which is the SDBS is the highest effective surfactant;
- Successfully study on using "green" - caffeine, reducing agent which has plant-source in synthesis rGO (graphene synthesized by chemical methods: reduced graphene oxide);
- - Systematic survey of catalytic synthetic methods Pt/rGO from different Pt precursors: H_2PtCl_6, $[Pt(NH_3)_4]Cl_2$, $[Pt(NH_3)_4](NO_3)_2$ and proved that with H_2PtCl_6, synthetic catalysts have a highest electrochemical activity and more efficient for the electrochemical oxidation of methanol reaction.

- Successfully synthesize the catalysts Pt-SiO_2/rGO and Pt-7% ASG have very high activity and particularly efficient activity. Compared with catalyst Pt/rGO not contain Al and Si, activity for the electrochemical oxidation of methanol reaction of these catalysts higher than 4.8 times, the stability against increase 1.3 times and time with stand prolonged poisoning than 6.3 times. The successful modification catalysts Pt/rGO by complex oxide AlOOH and SiO_2 contributes significantly reduce the amount of precious metals used in catalysts, resulting in lower cost of DMFCs;
- Tested in catalytic model DMFCs use Pt-7%ASG with negative density is 1 mg_{Pt}/cm^2, the battery has a capacity of 153 mW, performance transform chemical energy into electricity is 35.3%.

The research results have been published in 8 articles of academic international journals ISI and domestic magazines.

4. Layout of the thesis

The thesis consists of 111 pages (không kể phụ lục và tài liệu tham khảo) divided into sections: Introduction 2 pages, Chapter 1 Overview 26 pages, Chapter 2 Experiment 13 pages, Chapter 3 Results and Discussion 68 pages, Conclution 2 pages. The thesis consists of 7 tables, 72 pictures and photos and charts, 126 references.

B – MAIN CONTENT

CHAPTER 1: OVERVIEW

This chapter presents an overview of the fuel cell, DMFC fuel cells, graphene, Pt/graphene, Pt modified by various metals bearing on of graphene application in Direct Methanol Fuel Cell.

CHAPTER 2: EXPERIMENT

The experiments are performed in National Key Laboratory for Petrochemical and Refinery Technologies – Viet Nam Institue of Industrial Chemistry.

2.1. Preparation of catalysts

❖ **Preparation of graphene:** Graphene is synthesized by the method of mechanically separation using surfactants in combination ultrasonic vibration and chemical methods: Hummers improvement method.

- **Preparation of Pt/rGO:** the different mixed with slurry GO (graphene oxide), ultrasonic vibration, heat reflux, washed then dispersed in distilled water.
- **Preparation of Pt-M/rGO:** Methods of performing similar catalysts Pt/rGO but have added some metal salts.
- **Preparation of Pt-SiO_2/rGO:** Source materials used H_2PtCl_6, TEOS stirring with slurry GO then at 130^0C aging in teflon. The resulting mixture was washed and filtered with distilled water, alcohol and dried.
- **Preparation of Pt-AlOOH-SiO_2/graphene:** integrated similar to the catalytic Pt-SiO_2/ rGO but have additional aluminum tri - isopropoxide dispersed in isopropyl alcohol.

2.2. The catalytic characteristic methods

The catalysts are characterized by the modern physical and chemical methods such as: X-ray diffraction (XRD), Infrared spectroscopy (IR), Transmission electron microscope (TEM), Scanning electron microscope (SEM), Scanning electron microscopy combine with Energy-dispersive X-ray spectroscopy (SEM-EDX), High resolution transmission electron microscope (HRTEM), Therno Gravimetry/Differential Thermal Analyzer (TG/DTA), X-ray Photoelectron spectroscopy (XPS), Atomic Force Microscope (AFM), Raman, Inductively coupled plasma automic emission spectroscopy (ICP-OES).

2.3. Reviewed catalytic activity

The electrochemical measurements are performed on equipment PGS-IOC-HH12 Potentiostat/Galvanostat, with three electrode system in National Key Laboratory for Petrochemical and Refinery Technologies.

2.4. Experiment model DMFCs

Experimental models manufactured DMFCs are effected at the Corrosion and Protection of Metals, Materials Science Institute - Vietnam Academy of Science and Technology.

Test on a model initially DMFCs with size 7cmx7cm; cathode electrode is used as the cathode component is commercial Pt/carbon black carbon fabric coated on density 4 $mgPt.cm^{-2}$; anodic electrode using Pt-7% ASG carbon fabric coated on catalytic density: $1mgPt.cm^{-2}$.

Chapter 3: RESULTS AND DISCUSSION

3.1. Synthesis and characteristic properties of Graphene

3.1.1. Graphene synthesis by mechanical dissection method

The results characterized the microstructure properties of graphite and graphene synthesis from exfoliated graphite by mechanical delamination method (ultrasonic vibration) showed exfoliated graphite powder expanded structures with more sheets form graphite layer stacking to each other (Fig. 3.1a). The panels are of good size with many folds on the surface (Fig. 3.1b). Under the effect of ultrasonic vibration, the graphite layer is slowly peeling off, fewer at layer graphene (FLG) (Fig. 3.1c).

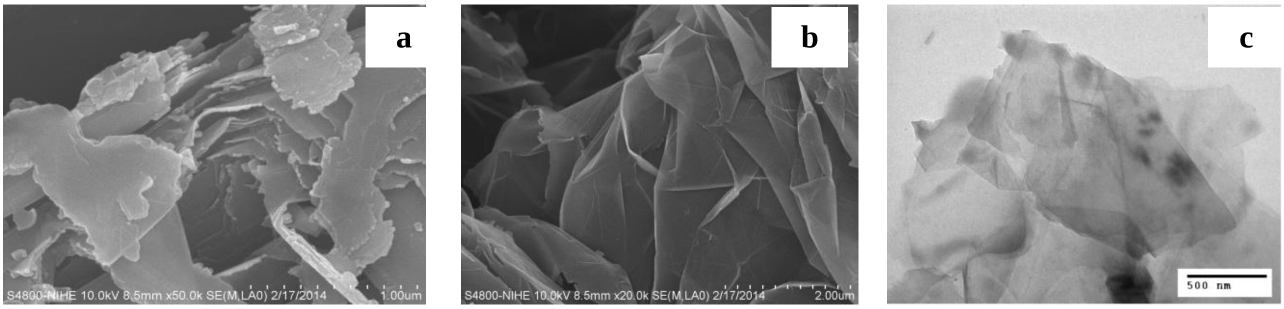

Fig. 3.1. SEM images of the exfoliated graphite powder (a), (b) and TEM image of FLG (c)

TEM images of the sample using FLG general ultrasonic vibration and various surfactants can see the level of exfoliated graphite powder thick ascending and descending plate FLG using water (Fig. 3.2a), NP-9 in water (Fig. 3.2b), CTAB in water (Fig. 3.2c) and SDBS in water (Fig. 3.2d). Thus, the ultrasonic vibration FLG samples in water containing CTAB and SDBS give better results than the synthetic form of water that does not contain surfactants and domestic contain NP-9. At the same time, demonstrated peeling degree of the samples in the same condition ultrasonic vibrations depends on distributed medium. Additionally, distributed environment can also affect the density dispersion and dispersion strength of domestic FLG.

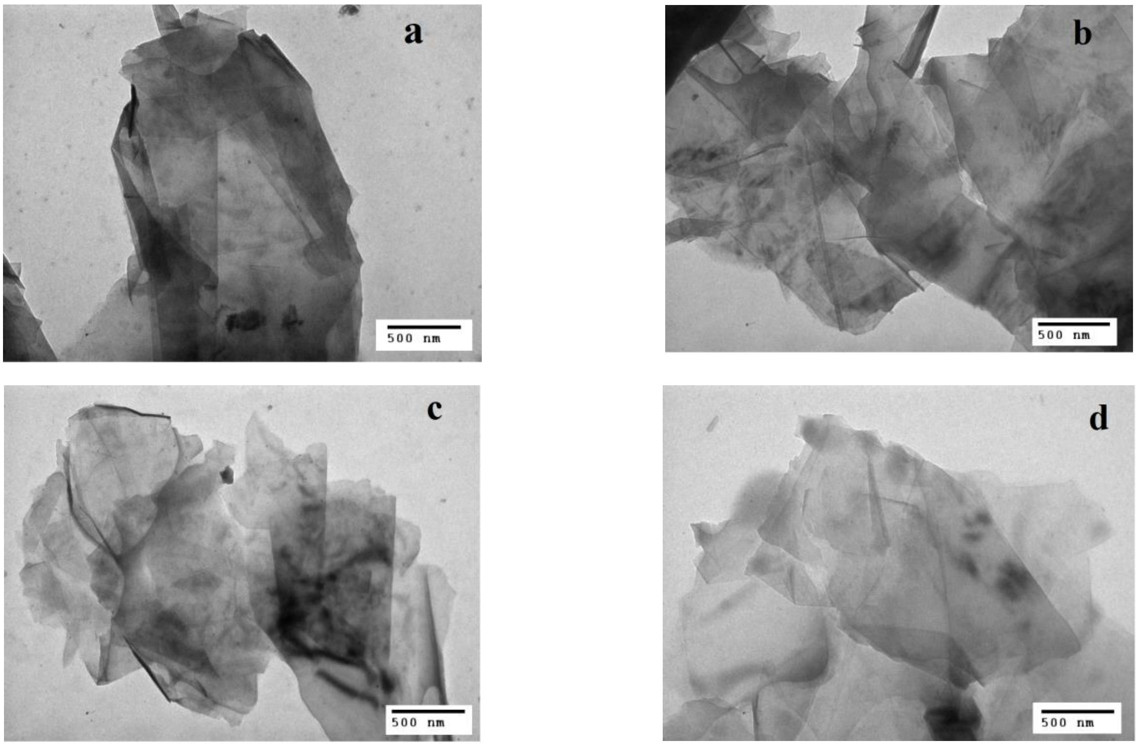

Fig. 3.2. TEM images of FLG synthetic in: water (a), NP-9 in water (b), CTAB in water (c) and SDBS in water (d

3.1.2. Graphene synthesized by chemical method

3.1.2.1. Characteristic properties of graphene synthesized by chemical method

Fig.3.4 shows that the microstructure rGO there are wide and thin membrane that almost transparent when viewed by transmission electron microscopy (TEM).

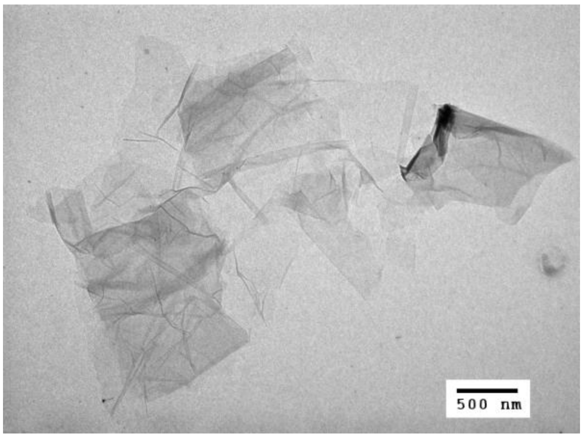

Fig. 3.4. TEM image of RGO

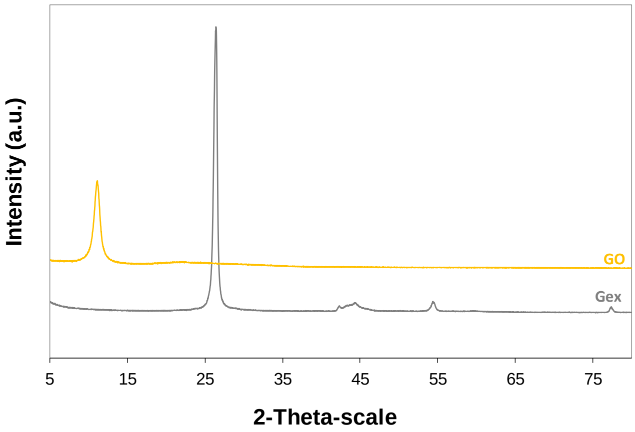

Fig. 3.5. XRD schema of exfoliated graphite (Gex) and graphene oxide (GO)

The results characteristic properties of exfoliated graphite (Gex) and graphene oxide (GO) by XRD method shows in Figure 3.5, on the graphene oxide XRD schema is no the typical peak of exfoliated graphite at position $2\theta = 26$, 45 and 55^{o}, but have a peak at 11^{o}, corresponding to the distance between the surface network is 8 Å, may now have functional groups oxidized graphene inserted between the plates. Thus, the XRD results demonstrated that the exfoliated graphite was completely transformed into graphene oxide.

The results characterized by Raman method shows in Figure 3.6, GO has band D intensity is much lower than the G band intensity ratio thus D/G ratio is less than 1. This is the mark indication of a decrease in the average size of sp2 domain. However, the Raman spectrum of the material showed D and G bands of rGO, in the position in 1350 and 1575 cm^{-1}respectively, with the D/G ratio is greater than 1. This demonstrates the presence many defects of the network (Csp3) after the reduction, which was synthesized by chemical methods.

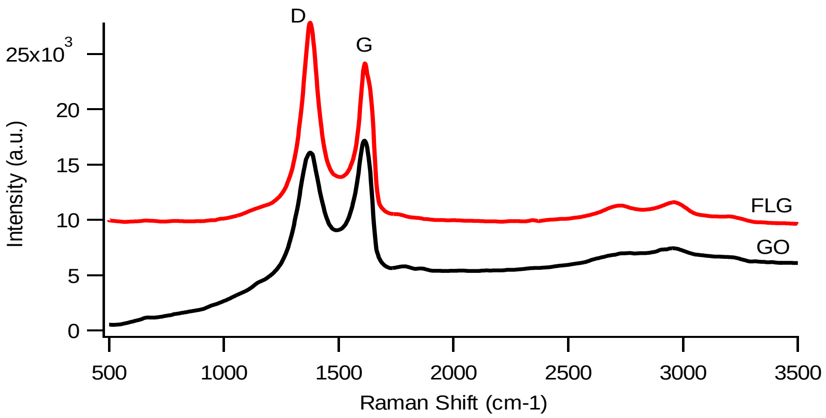

Fig. 3.6. Raman spectra of RGO

Observe the results determine the average layers of rGO by AFM method in Fig. 3.7 can be seen, the graphene sheets on SiO$_2$ substrate had average thickness of 2.4 nm (calculated from the difference between the surface elevation graphene sheet surface and substrate surface SiO$_2$). It is showed that the average thickness of the graphene monolayers at about 0.4 nm. So the average layers of the samples are prepared rGO is 6 layers.

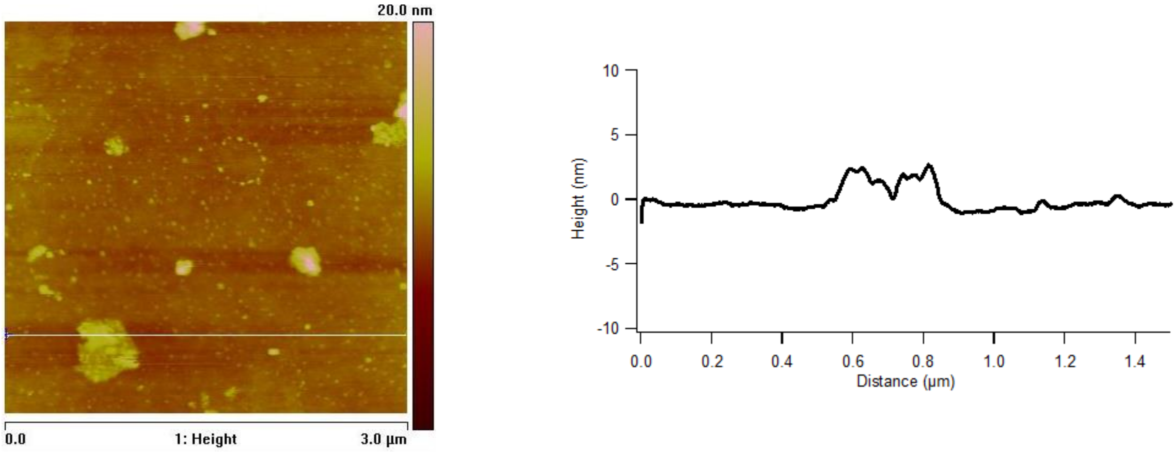

Fig. 3.7. AFM image and profile of sample rGO

3.1.2.2. The study used a reducing agent "green" in general RGO

Reducing agent "green" is mentioned in this study was caffeine. Figure 3.8 shows XRD patterns of raw graphite, GO and rGO. The complete transformation from GO to rGO is clearly illustrated by the disappearance of the 002 reflection line with no new diffraction peaks in the XRD pattern is obtained.

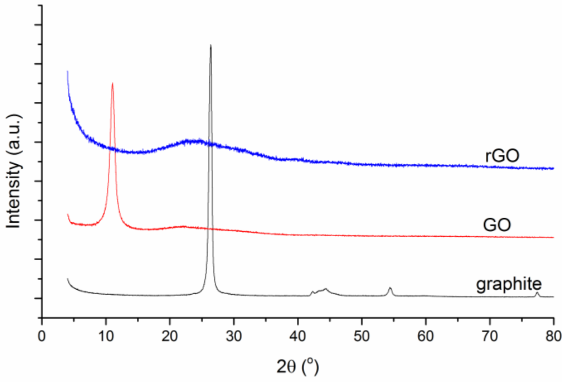

Figure 3.8. XRD spectra of graphite, GO and rGO.

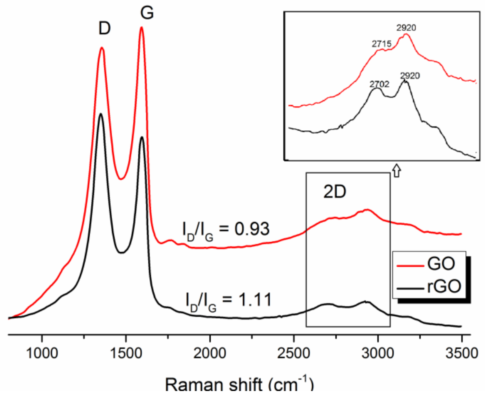

Figure 3.9. Raman spectra of GO and rGO.

Figure 3.9 illustrates the Raman spectra of GO before and after reduction with caffeine. the intensity ratio of the D and G band (*I*D/*I*G*)* of GO after reduction with caffeine increases from 0.93 (GO) to 1.11, indicating an increase in disordered domains during the reduction of GO. This change of *I*D/*I*G value is in good agreement with observations reported for the reduction of GO with hydrazine and other systems. In addition, it was noted that the 2D band of rGO shifted to 2702 cm−1 in comparison with that of GO observed at ~2715 cm−1. It was previously proposed that the reduction reaction favour the transformation of multilayer GO to further exfoli- ation into a fewer-layer or single-layer graphene. The band at ~2920 cm−1 was ascribed to the defect-related band.

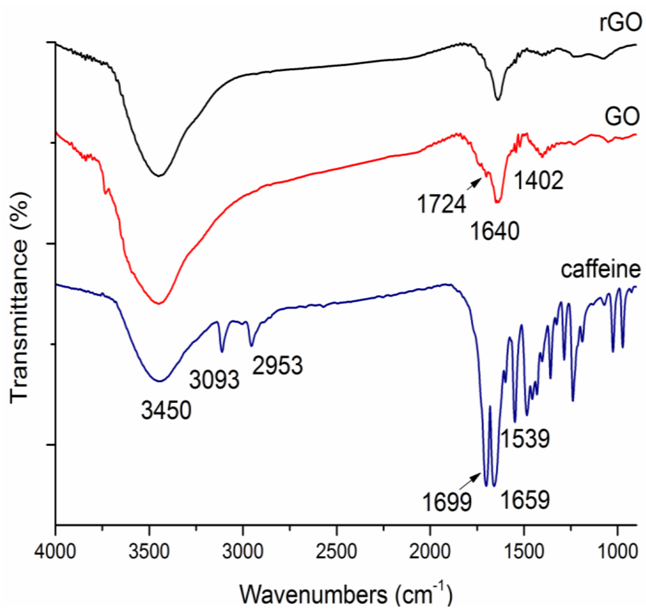

Figure 3. 10. FT-IR spectra of caffeine, GO and rGO

The FT-IR spectra of caffeine, GO and rGO are exhibited in figure 3.10, the FT-IR spectrum of rGO is quite similar to that of GO. However, the intensity of all the peaks correlated to the oxygen functional groups of rGO decreases dramatically Otherwise, the typical absorption bands of caffeine as well as any absorption bands of caffeine derivatives after reduction cannot be also observed in the FT-IR spectrum of rGO. These observations, therefore, could prove that most of oxygen-containing groups onto the GO nanosheets are removed in the reduction process using caffeine as the reducing agent.

In order to further illustrate the reduction extent of GO with caffeine, the C 1s XPS spectra of GO and rGO are used to prove the removal of the oxygen-containing groups (figure 3.11). In comparison to GO, the C 1s XPS spectrum of rGO shows a significant intensity decrease of C=O and C(O)OH bands and an appearance of C–O band indicating effective deoxygenation of GO after the chemical reduction. In addition, after reduction pro- cess, the surface C/O atomic ratio increases from 1.96 (GO) to 6.5 (rGO). These results show that the removal of oxygen- containing groups of GO using caffeine as reduction reagent was relatively successful.

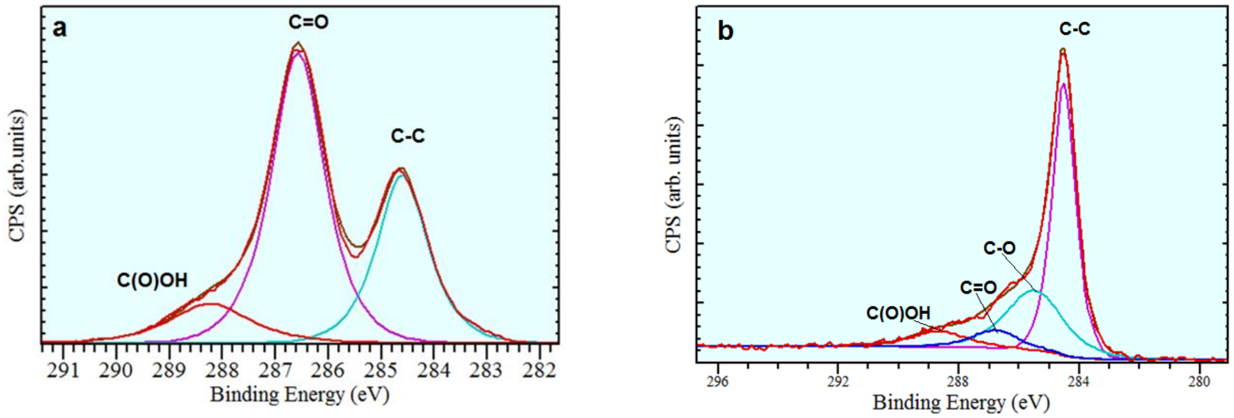

Figure 3.11. C 1s XPS spectra of (a) GO and (b) rGO

Thermal analysis results shown, after reduction, the rGO exhibit a reduced total weight loss compared to GO (28% weight loss). These results indicate an obvious decrease in the amount of oxygen-containing functional groups and a profound reduction of GO by caffeine. The results characterized the microstructure by TEM shown the part of graphene sheet shows relatively flat morphology with low contrast, indicative of few-layer thickness. Thus, the use of a reducing agent "green" GO eliminating initial positive results.

3.2. Catalyst Pt/rGO

3.2.1. Effect of different Pt precursors

Analytical results of Pt content, in the synthesized catalysts from different precursors by ICP-OES method in Table 3.1 indicates that the anion exchange between PtCl2- and the positively charged graphene oxide surface, dispersed suspensions in cloroplatinic acid solution may be the most effective way to attach Pt to the surface of graphene oxide.

Table 3.1. Pt content in the catalysts

Pt precursors	**Pt concentration of the exchanged solution (mol.g^{-1})**	**Pt concentration in catalysts (% weight)**
CPA (H_2PtCl_6)	0.008	21.7
TAPCl ($[Pt(NH_3)_4]Cl_2$)	0.015	10.5
TAPN($[Pt(NH_3)_4](NO_3)_2$)	0.008	10.5

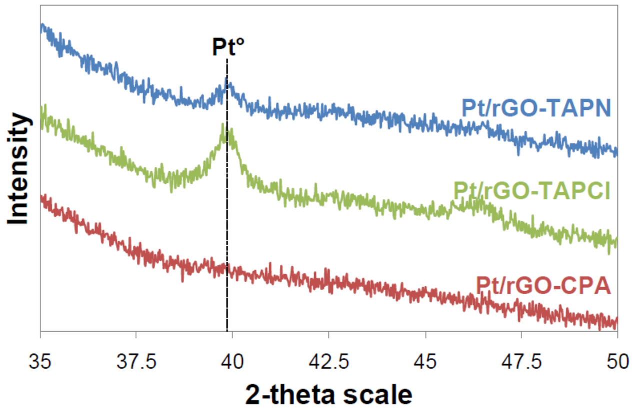

Fig. 3.14. XRD spectra of Pt/rGO catalysts

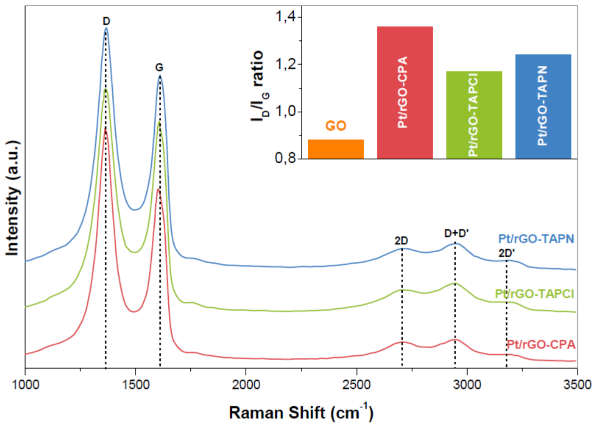

Fig. 3.14. Raman spectra of Pt/rGO catalysts

From XRD data (Figure 3.14) can classify the average size of the crystals depends on the used precursor Pt, in order of Pt/rGO-CPA < Pt/rGO-TAPN < Pt/rGO-TAPCl .

Raman spectra of the catalysts Pt/rGO-TAP, Pt/rGO-TAPCl and Pt/rGO-CPA (Figure 3.15) in the presence of D and G bands featured in the position 1350 cm$_{-1}$ and 1575 cm$_{-1}$, match with the characteristics of the material based on graphene.

The TEM images (Fig. 3.16) of three catalysts Pt/rGO makes it clear, there are two types of different microstructure dependent on the nature of the Pt precursors. When CPA precursor is used, the small size Pt particles (2-5 nm) distributed evenly over the surface of rGO. When tetraamin platinum precursor is used, the the small size Pt particles agglomerated into big size clumps Pt to 100 nm and more and seems to have weak links with rGO surface. Furthermore, in the reaction medium with ethylene glycol reducing agent, Pt precursors with high oxidation state (+4) as CPA can be reduced further than the other precursors and prevent from the formation of Pt subdivision large size.

XPS spectra of Pt 4f (Fig. 3.17b) includes typical peak of Pt$_0$ (60%) and partly oxidized Pt, Pt-OH (40%). This result demonstrates the reduction by EG is effective to reduce Pt/GO. In addition, the detailed analysis of C-OH signal and C(O)OH showed the functional groups cover about 23% of the surface compared with 10% for the rGO. Therefore, these results demonstrate that the conjugated carbon atoms in graphene network has been reduced in the synthesis of Pt/rGO as has been demonstrated from the results of XRD and Raman characterized.

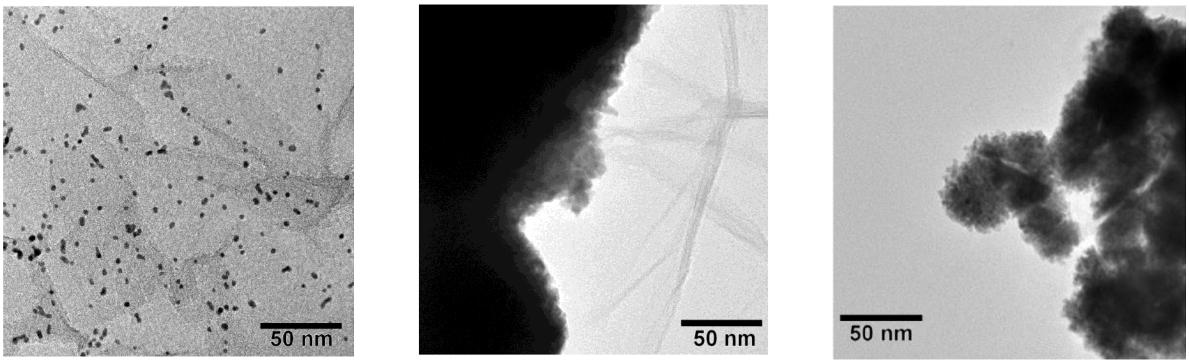

Fig. 3.16. TEM images of Pt/rGO synthesized from different Pt precursors *From left to right: CPA; TAPCl; TAPN*

The evaluation results of the catalytic activity in the oxidation of methanol consolidate that CPA precursor with high oxidation state (+4) is reduced further than other precursors have lower oxidation state, demonstrated that redox step is the most important step in the synthesis of catalysts Pt/rGO. CPA precursor is selected to synthesize catalysts based on Pt/rGO by method "wet impregnation" in the next studies.

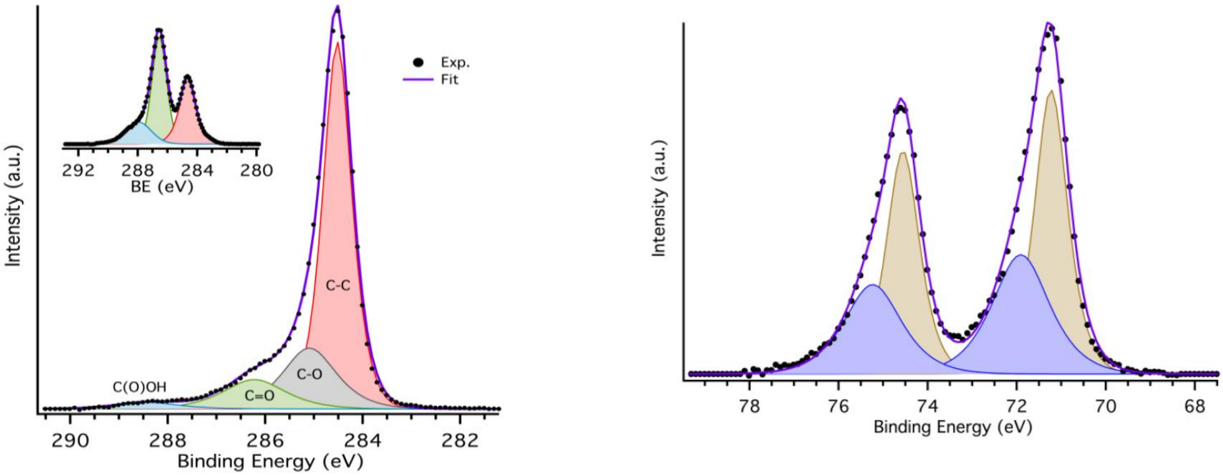

Fig. 3.17. XPS spectra of Pt/rGO-CPA: C(1s) (a) and Pt (4f) (b)

3.2.2. Effect of different reducing agents

Preliminary survey results show that catalysts Pt/rGO is synthesized with a reducing agent hydrazine hydrate much lower activity than samples synthesized with NaBH4 agents and EG. Therefore, these catalysts are not further study.

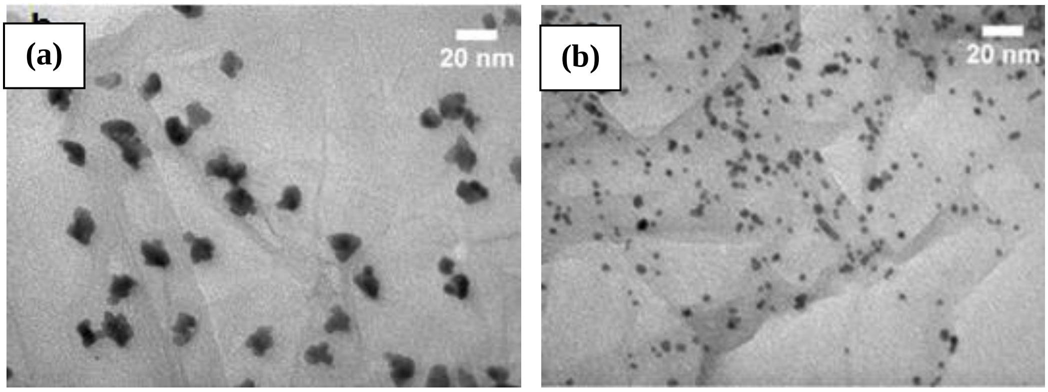

Fig. 3.21. TEM image of (a) Pt/ rGO-(NaBH$_4$) and (b) Pt/rGO-(EG)

The microstructure of the catalysts were prepared using the reducing agent NaBH$_4$ and EG are shown in Fig. 3.21.

With both catalysts, can observe characteristic structures of GO with thin sheets have good size, almost transparent, with rippled folds. For catalysts Pt/rGO- (EG) (Fig. 3.21b) can see the Pt particles evenly dispersed in the form of single particles on graphene, with sizes ranging from 2-7 nm, in which all is essentially about 2 nm particles, very few positions in which the particles are agglomerated to form "clusters" around 7 nm long rod. Meanwhile, the sample particles in a catalytic Pt Pt/rGO- (NaBH4) exists mostly as the "cluster" of several grain size from 3-8 nm (Fig. 3.21a). The "cluster" Pt particles are distributed relatively evenly over graphene sheets.

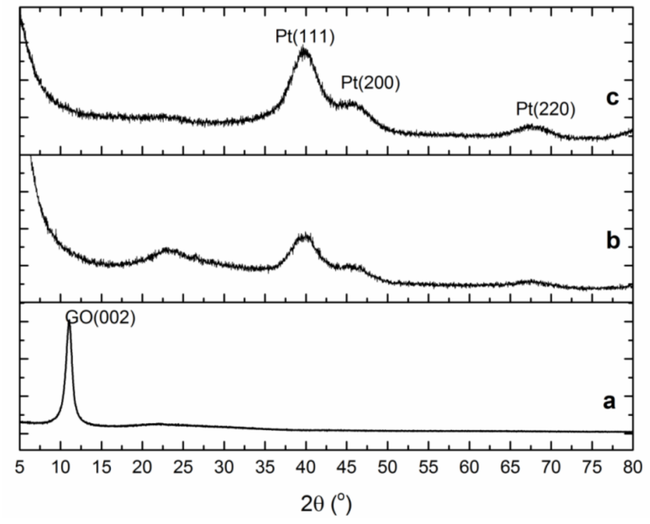

Fig. 3.22. XRD pattents of (a) GO, (b) Pt/rGO-(EG) and (c) Pt/rGO-(NaBH$_4$)

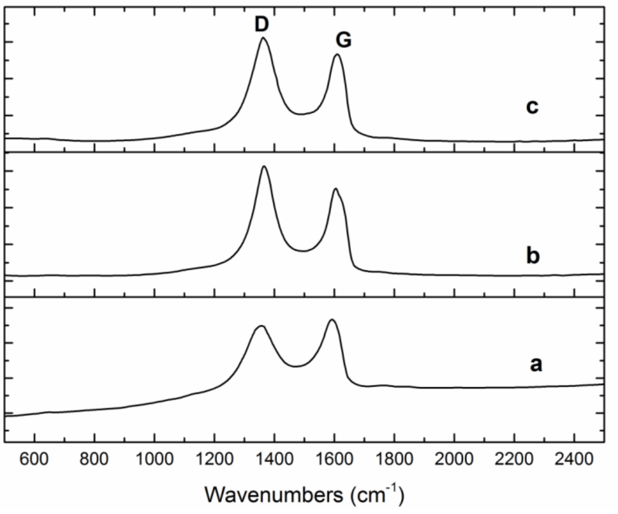

Fig. 3.23. Raman spectra of (a) GO, (b) Pt/rGO-(NaBH$_4$) and (c) Pt/rGO-(EG)

The XRD patterns of GO, Pt/rGO-(NaBH4) and Pt/rGO-(EG) samples are shown in fig. 3.22. In the fig. 3.22a, can obviously be seen the typical 002 reflection peak of GO at 11o. After the reduction, this peak is completely disappeared and a broad peak between 2ϴ = 24 - 26o (Fig. 3.22b and 3.22c) is observed indicating the graphene oxide is effectively reduced. In comparison with Pt/rGO-B catalyst (Fig. 3.22b), the intensity of Pt for Pt/rGO-A catalysts is more intense which results in the intensity decrease of graphene peak in Fig. 3.22c. These results reveal that the metallic Pt in the Pt/rGO-A sample may be higher than that in the Pt/rGO-B sample. These results are compatible with the findings of both the microstructure catalysts mentioned above.

Raman spectra of GO, Pt/rGO-A and Pt/rGO-B are shown in Fig. 3.23. In these spectra, the D band of graphene oxide exhibits a much lower intensity for the G band, so the D/G ratio is below 1, in good agreement with the Raman spectra of graphene oxide presented in the literature. This is the indication of a decrease in the average size of the sp2 domain. The Raman spectra of both Pt/rGO catalysts (Fig. 3.23b and 3.23c) have similar characteristics: the D and G bands are visible at 1350 and 1595 cm-1 and the D/G intensity ratio is above 1.0 that may be due to the defects (C sp3) after the reduction and the Pt nanoparticles on the graphene.

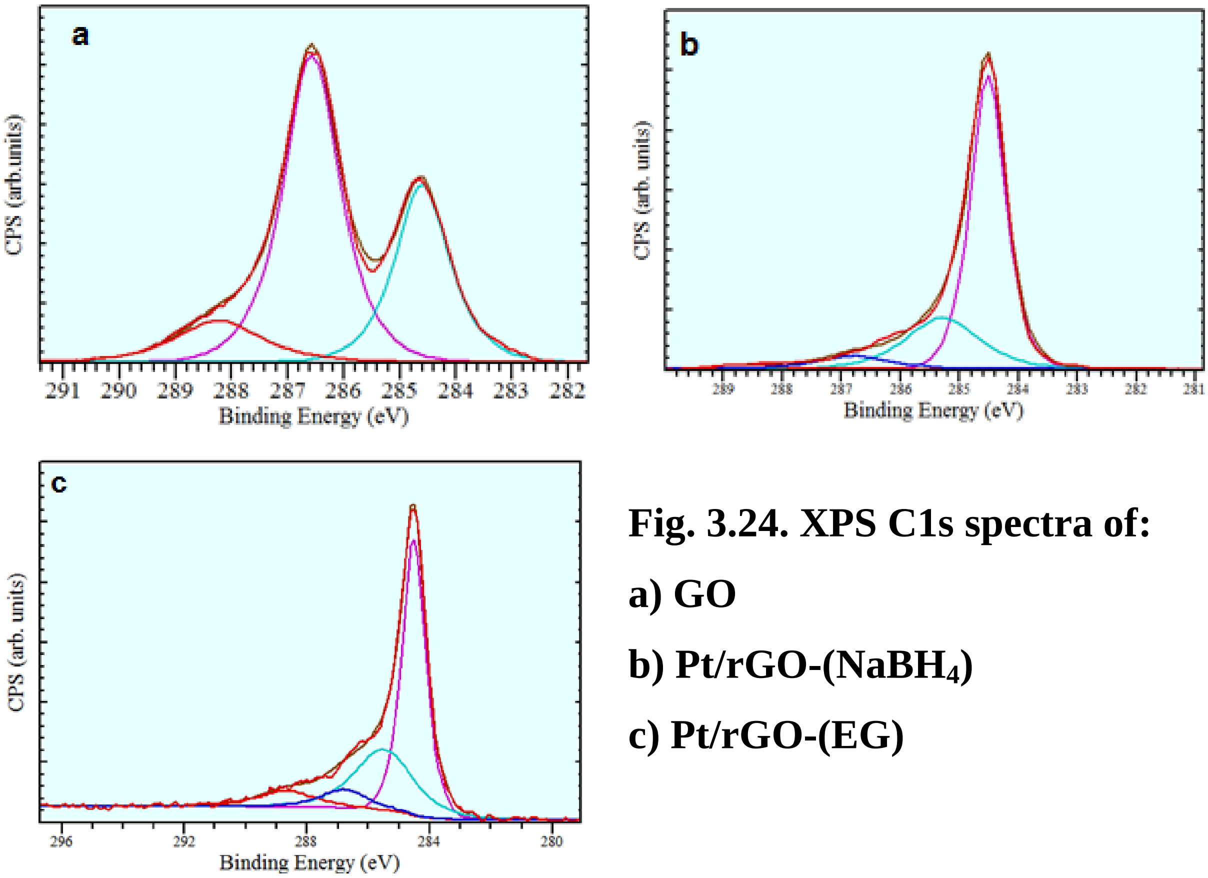

Fig. 3.24. XPS C1s spectra of:

a) GO

b) Pt/rGO-($NaBH_4$)

c) Pt/rGO-(EG)

The XPS spectra of GO, Pt/rGO-(NaBH4) and Pt/rGO-(EG) are shown in Fig. 3.24, The C–C/C–O peak intensity ratios in the Pt/rGO-(NaBH4) and Pt/rGO spectra obviously increase in comparison to that value of GO. This indicates that the oxygen-containing functional groups were removed during the reduction process, suggesting that GO was reduced.

The evaluation results of the catalytic activity in the oxidation of methanol showed that, although Pt/rGO- (EG) catalyst with the Pt particles with event dispersion and smaller than the size of Pt on the surface of the catalyst Pt/rGO-(NaBH4), electrochemical activity and durability of of Pt/ rGO-(NaBH4) is still higher than Pt/rGO-(EG) Pt because of the Pt total amount as well as the content of Pt (0) on the surface of Pt/rGO-(NaBH4) higher than Pt/rGO-(EG). Seem like EG has Pt capable dispersion in small sizes while NaBH4 has more effective than EG in bringing much Pt on rGO surface and especially reducing the Pt precursor into Pt0.

For these reasons, the reducing agent NaBH4 was used for subsequent experiments, involves studying the effects of Pt content to morphological and electrochemical activity of the catalysts Pt/rGO in electrochemical oxidation of methanol reaction.

3.2.3. Effect of Pt loading amount on morphology

The microstructure characterized results (Fig 3.27) and electrochemical activity survey results (Fig. 3.28) shows that sample 40% Pt/rGO is a catalyst which has average size of the Pt particles is low and these particles dispersed evenly on the graphene surface with the the best dispersion, so active and reactive highest reliability in the catalysts were investigated.

3.3. Modify Pt/rGO

The preliminary survey of the catalytic activity of Pt/rGO was modified by metals (Pd, Au, Ni, Rh, Sn, Ru), metal complexes (Pd-Au), oxide SiO_2, Al-Si oxide complex in the oxidation of methanol electrochemical (Fig. 3:29) shows, most, the modified catalysts are highly active, resistance to poisoning and reliability at much higher activity catalysts of Pt /rGO not denatured. In particular, the catalyst Pt / RGO be denatured by Ni or Ru active and durable, and the catalyst was modified by oxides Si or Si-Al complex oxide have active and super durability higher, than that of the catalysts have been published to date. Because there are interesting results, the catalyst Pt/rGO was modified by Ni, Ru, Si oxide or Al-Si oxide complex will be studied in detail.

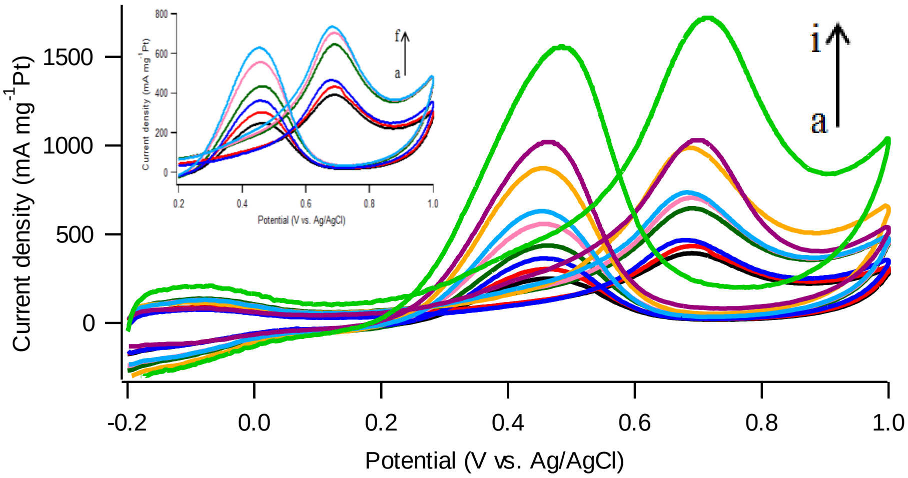

Fig. 3.29. CV of catalysts at scan rate of 50 mV.s^{-1}: a) Pt-Au/rGO, b) Pt-Pd/rGO, c) Pt-Au-Pd/rGO, d) Pt-Sn/rGO, e) Pt-Ni/rGO, f) Pt-Rh/rGO, g) Pt-Ru/rGO, h) Pt-SiO_2/rGO2 and i) Pt-7%ASG

3.3.1. Modify by Ni and Ru

The results of the structural characteristics and evaluation of the catalytic activity in the electrochemical oxidation of methanol demonstrate the positive impact of the promotion phase M (Ru, Ni) on catalytic Pt / RGO.

3.3.2. Modify by Si

To assess the role of denaturant SiO2, in this content Pt/rGO catalysts was modified by SiO2 with different content (theoretical calculation) respectively 7%, 11% and 17%. To briefly in the presentation, these catalysts are denoted as: Pt-SiO2/rGO1, Pt-SiO2/rGO2 and Pt-SiO2/rGO3.

Structural characteristics of GO, SiO2/rGO, Pt/rGO and Pt-SiO2/rGO2 is presented in Fig. 3.37, 3.38, 3.39 and 3.40. Electrochemical catalytic activity of these catalysts are summarized in Table 3.5 .

These results demonstrate nanocomposite Pt-SiO_2/rGO2 with electrochemical catalytic activity and the best resistance to poisoning among the catalysts Pt-SiO_2/rGO.

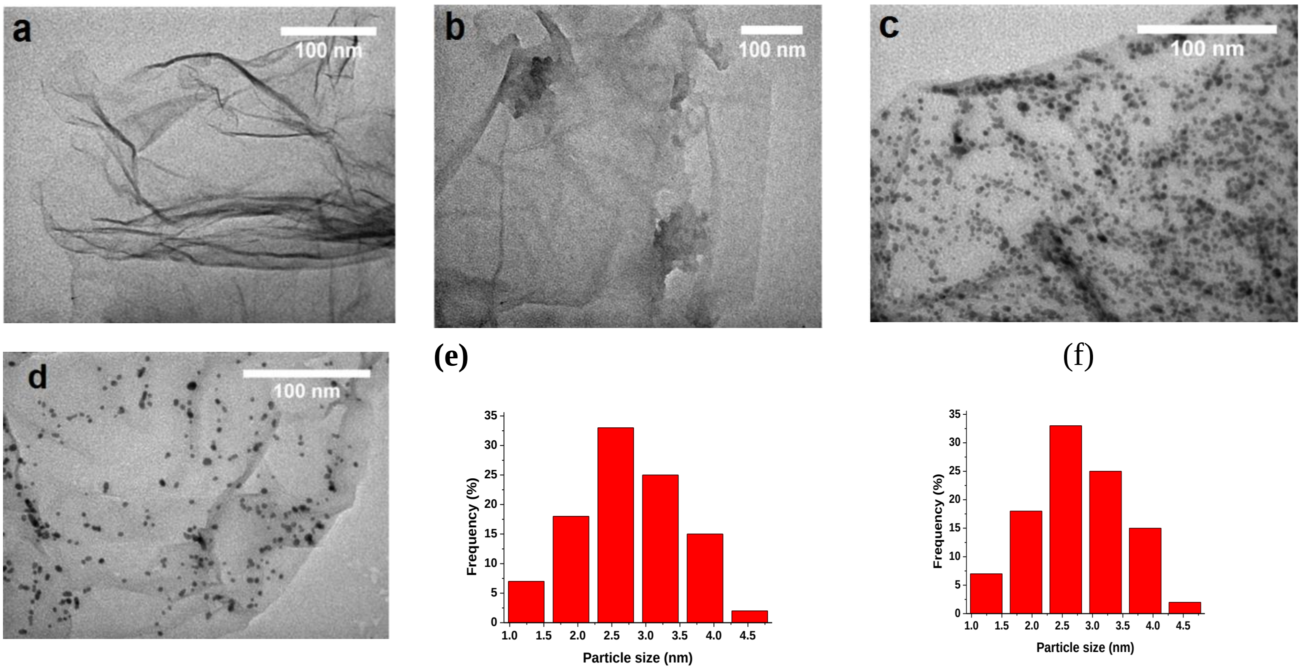

Fig. 3.37. TEM images of a) GO, b) SiO_2/rGO, c) Pt-SiO_2/rGO2, d) Pt/rGO and Pt particle size distribution of: e) Pt-SiO_2/rGO2, f) Pt/rGO

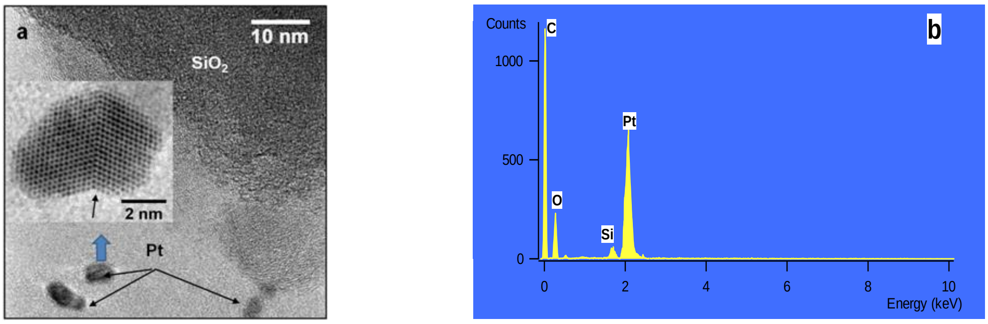

Fig. 3.38. a) HR-TEM image and b) EDS of Pt-SiO_2/rGO2

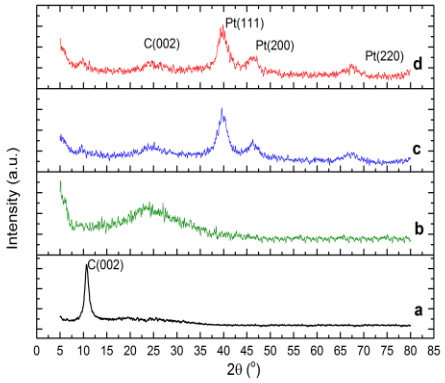

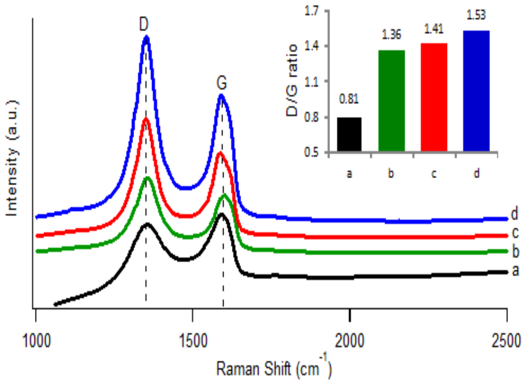

Fig. 3.39. XRD patterns of a) GO, b) SiO_2/rGO, c) Pt-SiO_2/rGO2 and d) Pt/rGO

Fig. 3.40. Raman of a) GO, b) SiO_2/rGO, c) Pt/rGO and d) Pt-SiO_2/rGO2

Table 3.5. Compare electrochemical activity of the catalysts modified by SiO_2

Catalyst	ECSA (m2/g)	IF (mA.mg-1Pt)	IR (mA.mg-1Pt)	IF/IR
Pt-SiO2/rGO2	87,19	1047	1010	1,04
Pt-SiO2/rGO1	62,53	520	483	1,08
Pt-SiO2/rGO3	51,30	320	313	1,02
Pt/rGO	41,19	248	225	1,10
SiO2/rGO	-	-	-	-

These results demonstrate nanocomposite Pt-SiO_2/rGO2 with electrochemical catalytic activity and the best resistance to poisoning among the catalysts Pt-SiO_2/rGO.

3.3.3. Modify by Si-Al

Fig. 3.48 shows the XRD patterns of GO, ASG, Pt-G and Pt-7%ASG. It is obvious that the spectra of GO exhibits the typical reflection peak of GO (002) at 10.6○ (Fig. 3.48a). As displayed in Fig. 3.48b-d, after the reduction reactions, the peak of graphene oxide is not observed anymore and the diffraction patterns show broad peak around 2q ¼ 24○ which is the characteristic (002) peak of graphene nanosheet.

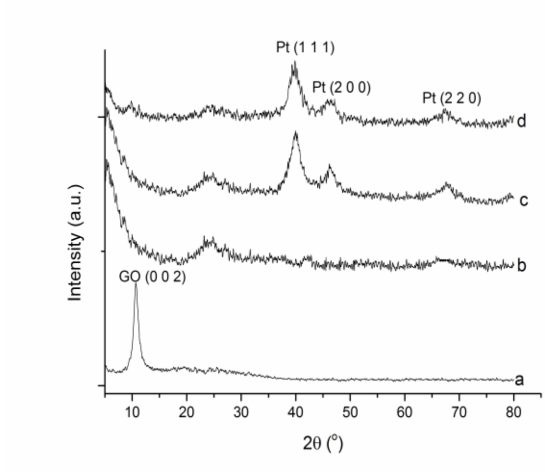

Fig. 3.48. XRD patterns of a) GO, b) ASG, c) Pt-7%ASG and d) Pt/rGO

In the XRD spectra of ASG and Pt-7%ASG hybrids, the diffraction peak at 24÷26○ is also attributed to the signal of amorphous silica which makes the intensity of this signal higher compared to Pt/rGO. It is remarkable that no diffraction peaks corresponding to the aluminum based compounds are observed in Fig. 3.48b and c indicating that AlOOH exists in either amorphous or nanocrystalline particles in hybrid materials.

The morphology, the size, and the dispersion of Pt catalysts were examined by TEM and HRTEM (hình 3.49 và 3.50).

In order to determine optimal Al, Si dopant amount on graphene for methanol oxidation, electrochemical measurements were carried out on catalysts with various total contents of Al and Si elements (4%, 7% and 10%) and the same 40% Pt loading (the ratio according to theoretical calculations, compared with the weight of rGO).

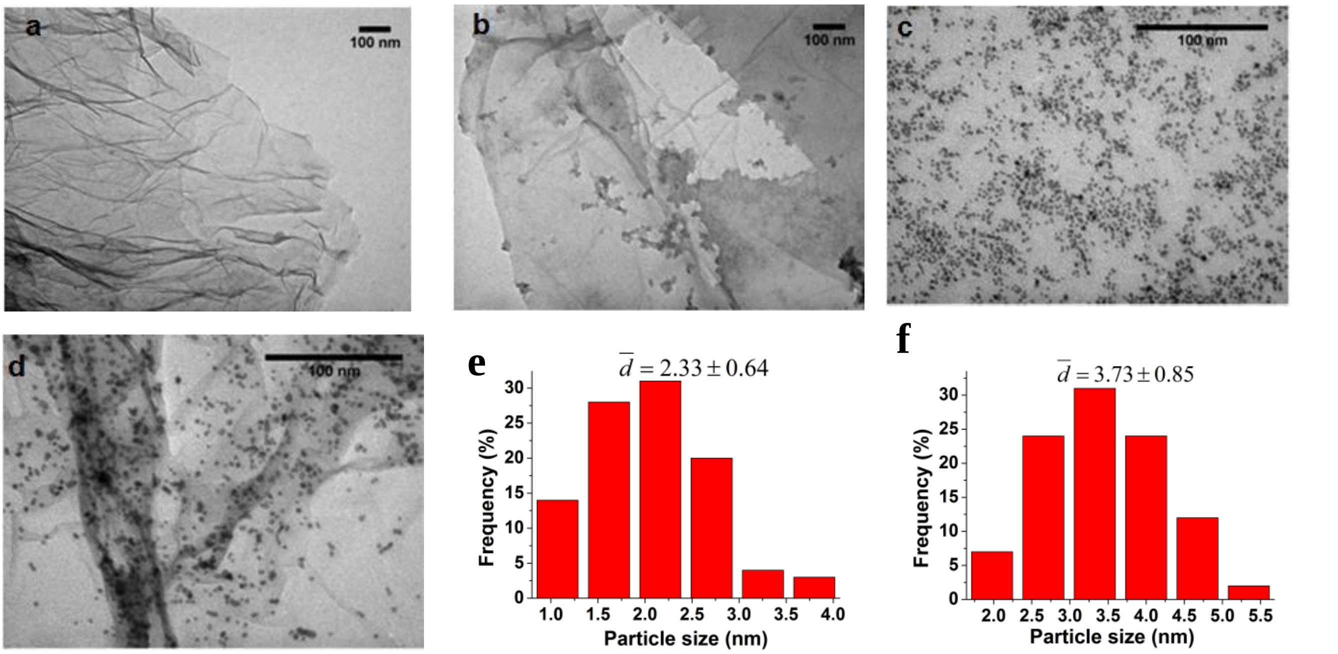

Fig. 3.49. TEM images of a) GO, b) ASG, c) Pt-7%ASG, d) Pt/rGO and Pt particle size distribution of e) Pt-7%ASG, f) Pt/rGO

These TEM and HRTEM analysis have shown the improvement of Pt nanoparticles dispersion on the graphene nanosheets for Pt-7% ASG.

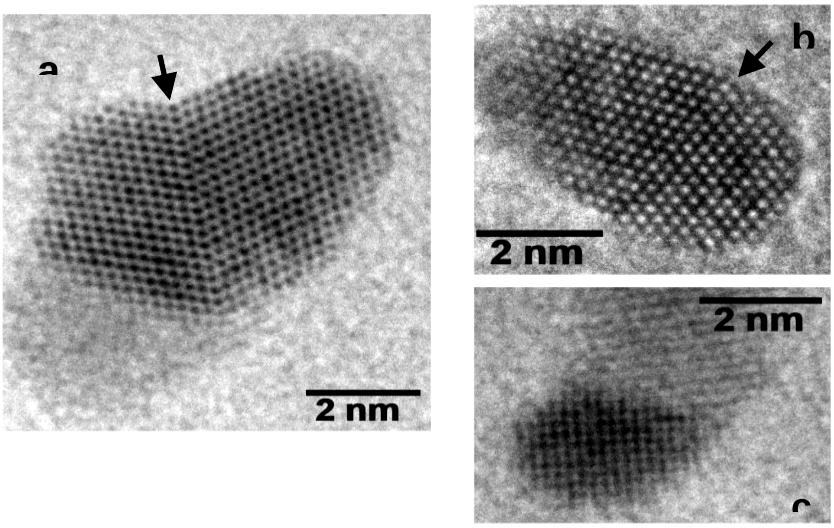

Fig 3.50. HRTEM images of Pt-7%ASG catalyst with nanoparticles partially oriented: (a-b) in the (110) direction and (c) in the (001) direction

The cyclic voltammograms of the catalysts with different doping amounts in 0.5 M H_2SO_4 solution are shown, material ASG no catalytic activity. The CV curves of Pt-G and Pt-ASG with different Al, Si contents show clear H_2 adsorption/desorption peaks in the potential range from - 0.2 to 0.1 V (vs. Ag/AgCl). The calculated results are given in table 3.7.

It s note that, the ECSA of the Pt-ASG catalyst is increased with the increase of the Al, Si content up to 7%. At this optimal doping content, the largest ECSA value equals 116.3 $m^2.g^{-1}$, which is 2.6 times higher than that of Pt/rGO (44.0 $m^2.g^{-1}$). Also, the value is the higher than those measured on other Pt-based catalyst, including Pt/graphene (53.9 $m_2.g_{-1}$), Pt-CeO_2/GN (66.4 $m^2.g^{-1}$), Pt/MnO_2/GS (103.2 $m^2.g^{-1}$), Pt/TiO_2/graphen (96.7 $m^2.g^{-1}$).

Table 3.7. Compare electrochemical activity of the catalysts modified by Al and Si complex oxide

Catalyst	**ECSA ($m^2.g^{-1}$)**	**I_F ($mA.mg_{Pt}^{-1}$)**	**I_R ($mA.mg_{Pt}^{-1}$)**	**I_F/I_R**
Pt-7%ASG	116,31	1720	1560	1,10
Pt-4%ASG	81,80	259	101	2,56
Pt/rGO	44,00	250	208	1,20
Pt-10%ASG	41,50	161	143	1,12
ASG	-	-	-	

In this work, the different ECSA values of the catalysts with the same Pt loading should be due to the effect of different AlOOH, SiO2 contents on the Pt dispersion and the conductivity of the support. With the increase of the Al, Si content to 7%, the Pt particles were highly dispersed with smaller particle sizes, thus the ECSA was increased. Nevertheless, when the Al, Si content is 10%, the conductivity of the support was largely affected, thus the ECSA was reduced. Herein, the best Al, Si content of the hybrid material is 7%.

These results (Fig. 3.53, 3.54, 3.55) provide further evidence that the Pt-7%ASG hybrid has the best electrocatalytic property and antipoisoning ability among the four catalysts. .

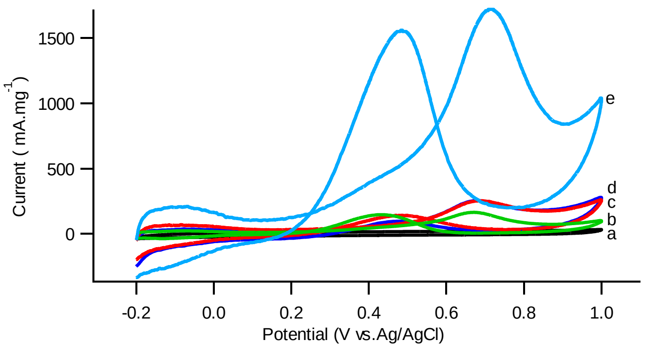

Fig. 3.53. CV curves of catalysts in 0.5 M H_2SO_4 + 1 M CH_3OH solution at scan rate of 50 mV.s^{-1}: a) ASG, b) Pt-10%ASG, c) Pt/rGO, d) Pt–4%ASG, e) Pt–7%ASG

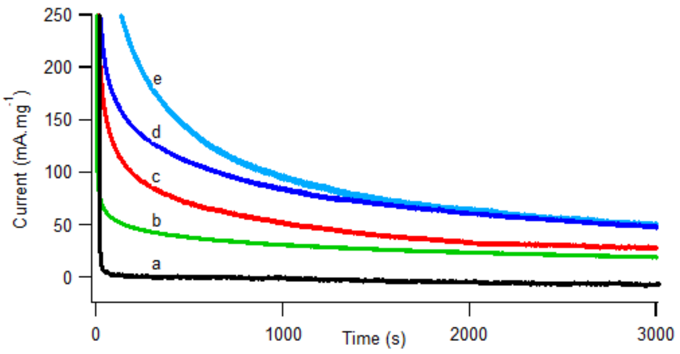

Fig. 3.54. CA curves of catalysts at potential of 0,7 V: a) ASG, b) Pt-10%ASG, c) Pt/rGO, d) Pt-4%ASG and e) Pt-7%ASG

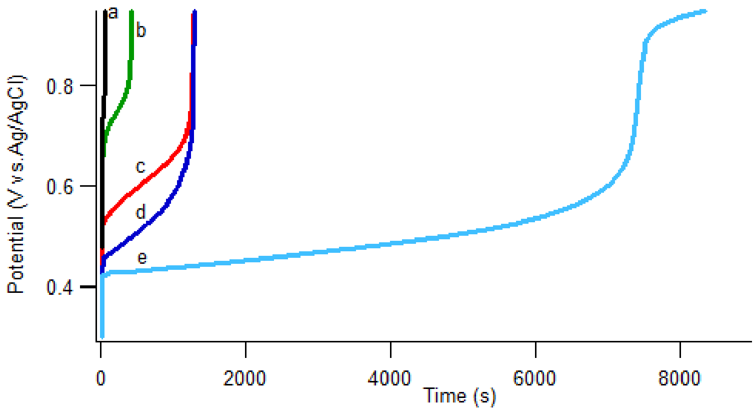

Fig. 3.55. CP curves of catalysts at curent density of 1.1 mA.cm^{-2}: a) ASG, b) Pt-10%ASG, c) Pt/rGO, d) Pt-4%ASG and e) Pt-7%ASG

Pt-ASG electrocatalysts were successfully synthesized by a one - pot method. The Pt nanoparticles were highly dispersed on the surface of graphene sheets with average particle size of 2.3 nm against 3.7 nm for the Si, Al free Pt-G. Especially, hybrid nano - material containing 7% total amount of Al, Si exhibits extremely high electrocatalytic performance, good antipoisoning ability and exceptional long-term stability. Compared to the Si, Al free Pt/graphene catalyst, the activity toward methanol electrooxidation on this catalyst was improved by 4.8 times; the stability for methanol electrooxidation also increased by1.3 times and the sustained time was significantly prolonged by 6.3 times. In conclusion, the Pt-AlOOH-SiO2/graphene hybrid could be used as an effective catalyst for DMFC. Catalyst Pt-7%ASG is selected as catalyst to manufacture DMFCs.

3.4. Effect of electrochemical medium

Effect of electrochemical medium was made on glassy carbon electrode with catalyst Pt- 7% ASG.

3.4.1. Effect of methanol concentration

Survey results showed that the concentration of methanol 2 M is suitable for electrochemical oxidation of methanol on selected catalysts.

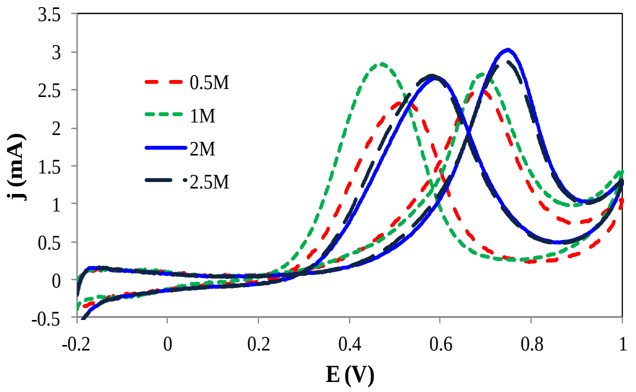

Fig. 3.56. CVcurves with rate scan 50 mV/s at different methanol concentration

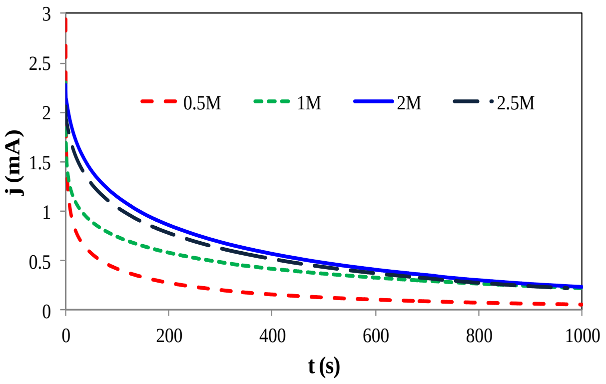

Fig. 3.57. CA curves with different methanol concentration

3.4.2. Effect of electrolyted medium

The survey results demonstrate, the suitable medium for electrochemical oxidation of methanol was acid medium.

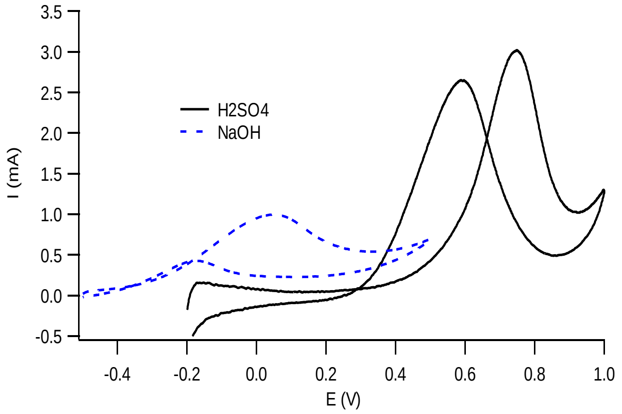

Fig. 3.58. CV curves with rate scan 50 mV/s at different electrolyted media

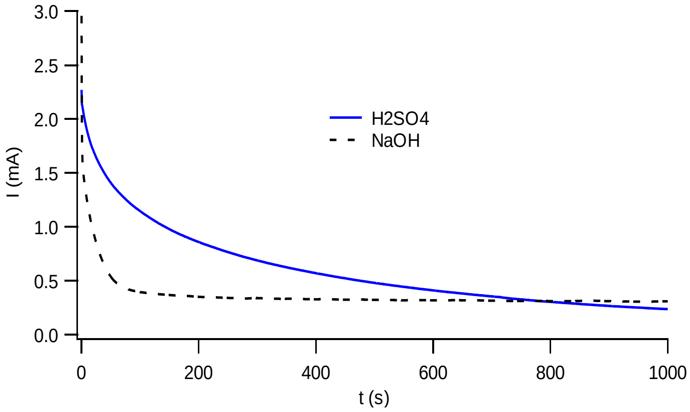

Fig. 3.59. CA curves with different electrolyted media

Applying this result to fabricate pin models, solid electrolyte acidic, proton transport only H^+, was chosen to make the electrolyted medium in DMFCs.

3.4.3. Effect of temperature

Survey results effect of temperature showed that the ambient temperature is selected as the operating temperature of the DMFC battery models.

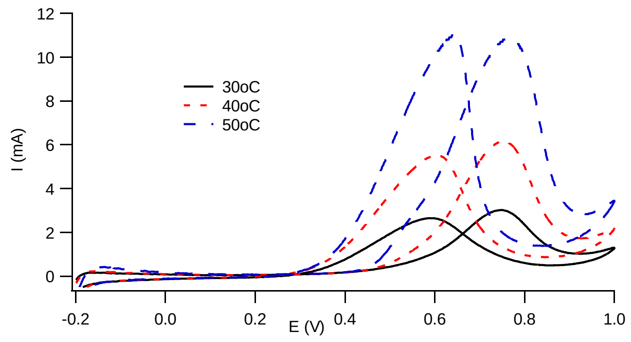

Fig. 3.60. CV curves with rate scan 50 mV/s at different temperature

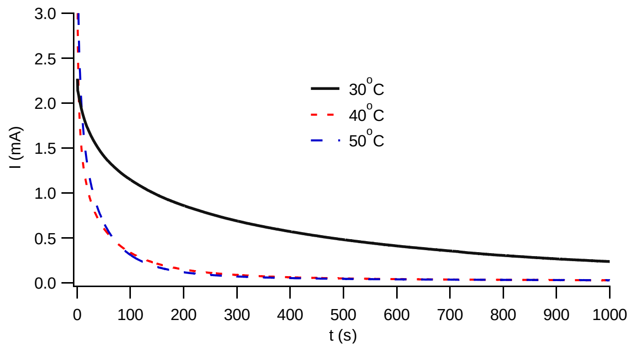

Fig. 3.61. CA curves with different temperature

4. Experiment DMFC models

The theoretical capacity of the model 7cm x 7cm (anode electrode using Pt-7% ASG coated carbon fabric on density catalysts: 1 $mg_{Pt}.cm^{-2}$) is 158 mW. Power value measured on the model very close to the theoretical value, approximately 153 mW (Fig. 3.62).

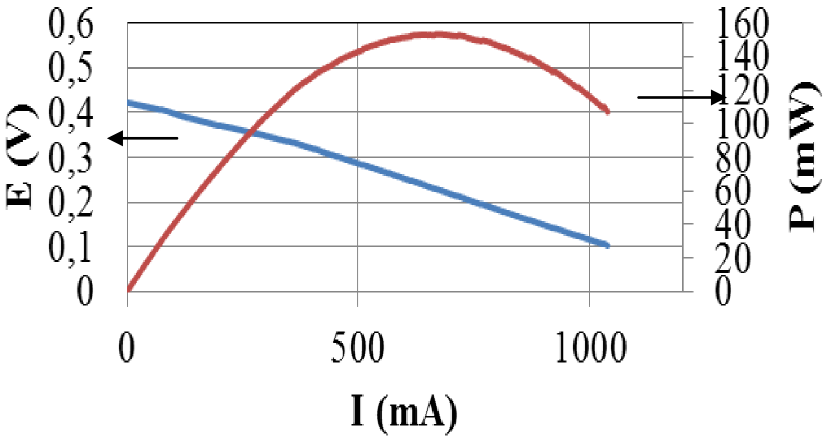

Hình 3.62. E-I curve and curve of the model 7 cm x 7 cm battery

Measurement results equivalent electric battery model 7 cm x 7 cm at 0,3V voltage after time result 4h total actual equivalent electricity in battery voltage is 0,3V 1,652,247 (mC) or 1652247 (mA.s).

Calculation results show that the efficiency of conversion of chemical energy to electrical energy is 35.3% battery..

CONCLUSIONS

1. Successfully synthesized graphene by two different methods: a mechanical delamination method and chemical methods. Both methods allow to synthesize few layer graphene (under 10 layers);

2. Successfully study on using "green" - caffeine, reducing agent which has plant-source in synthesis rGO;

3. Systematic survey of catalytic synthetic methods Pt/rGO from different Pt precursor sources: H_2PtCl_6, $[Pt(NH_3)_4]Cl_2$, $[Pt(NH_3)_4](NO_3)_2$ and proved that with H_2PtCl_6 have high oxidation state (+4) is reduced further than other precursors have lower oxidation state show that redox step is the most important step in the synthesis of Pt/rGO and prevent the formation of larger Pt particles so catalytic activity is the highest electrochemical activity and more stability activity for the electrochemical oxidation of methanol reaction.

4. Systematic survey of "Wet impregnation method" for preparing catalysts Pt/graphene and identifiing the appropriate conditions to obtain the catalyst with Pt content of 22.10 wt% and the size of Pt particles of about 10-13 nm are: catalysts Pt/rGO is synthesized from the precursor H_2PtCl_6 with theoretical content of 40%, using a step reduction process with the reducing agent NaBH4.

5. Studied on modifiing Pt/rGO catalysts by metals Au, Pd, Sn, Rh, Ru, Ni, Si, Si-Al and identified the modified catalysts based on AlOOH and SiO_2 (Pt-7%ASG) have very high activity and more stability of activity. The modification by AlOOH and SiO_2 are improves the dispersion of Pt particles on the surface of graphene sheets so increase the ratio of Pt contact to oxygen. On the other hand, the modification can create a medium of priorities for the adsorption of methanol on the surface of catalysts, leads to synergistic effects with Pt to promote the reaction. Compared with catalyst Pt/rGO not contain Al and Si, activity for the electrochemical oxidation of methanol reaction of these catalysts higher than 4.8 times, the stability against increase 1.3 times and time with stand prolonged poisoning than 6.3 times.

6. The results of the survey some elements of the electrochemical medium to catalytic activity such as methanol concentrations, electrolyte medium and temperature showed that the concentration of methanol 2 M; electrolyte

medium of H_2SO_4 0.5 M and 30°C are suitable conditions for methanol oxidation catalysts.

7. Tested in catalytic model DMFCs used Pt-7%ASG with negative density is 1 mg_{Pt}/cm^2, the battery has a capacity of 153 mW, performance transform chemical energy into electricity is 35.3%.

LISTS OF RELATED ARTICLES OF THESIS

1. Ảnh hưởng của Ru, Ni như chất xúc tiến đến hoạt tính điện hóa của xúc tác Pt/rGO đối với phản ứng oxi hóa metanol. *Tạp chí Hóa học*, 2014, 52(6B), 46-49.
2. “Facile and efficient single-step preparation of Pt/graphen catalysts with improved methanol electrooxidation activity”. *The Second International Workshop on Nano Materials for Energy Conversion, Ho Chi Minh City, Vietnam*, 2014.
3. Pt-AlOOH-SiO_2/graphen hybrid nanomaterial with very high electrocatalytic performance for methanol oxidation. *Journal of Power Sources*, 2015, 276, 340-346.
4. Solvothermal synthesis of Pt-SiO_2/graphen nanocomposites as efficient electrocatalyst for methanol oxidation. *Electrochimica Acta*, 2015, 161, 335-342.
5. Synthesis of Pt/rGO catalysts with various reducing agents and their methanol electrooxidation activity. *Materials Research Bulletin*, 2016, 73, 197-203.
6. A new green approach for the reduction of graphen oxide nanosheets using caffeine. *Bulletin of Material Science*, 2015, Vol. 38, No. 3, 667-671.
7. Nghiên cứu ảnh hưởng của môi trường phân tán trong quá trình điều chế graphen ít lớp (FLG) bằng phương pháp rung siêu âm. *Tạp chí Hóa học và Ứng dụng*, 2015, 1(29), 60-62 và 80.
8. Khảo sát hoạt tính oxi hóa điện hóa metanol của xúc tác Pt/rGO biến tính, ứng dụng cho pin DMFC. *Tạp chí Hóa học*, 2015.